Electron Localization in Metallic Quasicrystals

F. S. Pierce, S. J. Poon,* Q. Guo

Bulk icosahedral-quasicrystalline aluminum-palladium-rhenium alloys of high structural quality and thermal stability are found to exhibit low-temperature electrical resistivities that are four orders of magnitude larger than those found in disordered metals and metallic glasses. Experiments suggest that these quasiperiodic alloys, which have a semimetallic electron density, are insulators at low temperature. The findings are discussed in light of theories on electron localization and band-gap formation in ordered metallic systems.

The discovery of icosahedral-phase (*i*-phase) alloys (*1*), a class of solid-state structures known as quasicrystals (*2*), has spawned the search for effects attributable to quasiperiodicity that influence condensed-matter properties (*3, 4*). Among the latter, electronic properties of quasicrystals are expected to be different from those of crystalline and amorphous solids. This is because the competition between localization and delocalization in a quasilattice, which are caused by nonperiodicity and self-similarity, respectively, can lead to electronic states that are critical—that is, neither localized nor extended (*5*). It has also been shown that transition to the localized state in quasicrystals takes place as the strength and complexity of atomic potentials increase (*5–7*). The latter condition can be realized in alloy systems. Naturally, these solid-state structures have prompted many experimental endeavors (*3, 4, 8, 9*). In addition to the fundamental issues of interest, the observation of Anderson localization in an ordered metallic phase will be intriguing in its own right because the metal-insulator transition has been studied mostly in nonmetallic and metal-oxide-granular systems (*10*).

The initial groups of *i*-phase alloys studied were structurally disordered (*11*); their electronic properties were found to be similar to those seen in amorphous metals (*8, 9*). Since 1987, the discovery of a series of thermally stable quasicrystals (*12*) that are highly ordered (*13*) has provided an impetus for exploring the intrinsic properties of quasiperiodic alloys. Indeed, studies made on the new systems in the past 3 years have indicated the precursor to electron localization (*14–17*). First, low-temperature resistivities (ρ) at 4.2 K that are two orders of magnitude larger than those seen in amorphous metals have been measured in *i*-AlCuRu (*14*), AlCuFe (*15*), AlPdMn (*16*), and AlPdRe (*17*) alloys. These alloys are typically composed of 60 to 70 atomic percent Al and approximately 20 atomic percent Cu or Pd. A strong temperature dependence of ρ, as seen in the resistivity ratio $R = \rho(4.2\ \mathrm{K})/\rho(290\ \mathrm{K}) \sim 2$ to 10 compared with $R < 1.2$ for amorphous metals, is also measured [see references and notes for maximum $\rho(4.2\ \mathrm{K})$ and R reported for each alloy system]. Analysis based on Boltzmann transport, which takes into account the carrier densities (*14, 15*) shows that the electron mean free path is much shorter than the Fermi wavelength (*9*). Finally, the optical conductivity is non–Drude-like (*18*). These findings indicate that the ordered quasicrystals lie outside the realm of metallicity (*10*). There have even been some speculations about semiconducting quasicrystals (*19*).

We present in this report *i*-phase alloys of AlPdRe that show low-temperature resistivities reaching ~1 ohm-cm and temperature dependence resembling that of an insulator. The density of electrons at the Fermi level is that of a semimetal (~10^{20} cm^{-3}). Our findings, which are consistent with the picture of Anderson localization, are unusual for a system based on good metals. The realization of our new results can be attributed to the high structural quality of the samples. Specifically, the purity of both the initial and final products is crucial, particularly so because the chance that the impurity phases in a metal-based system are "good conductors" is very high. Polycrystalline Al-Pd-Re ingots (Table 1) were prepared by melting high-purity elements, under argon in an arc furnace. Samples for study were cut from ingots, in well-defined geometrical shapes with dimensions ~1 mm × 1.5 mm × 6 mm, and then annealed in good vacuum at 860° to 950°C for 12 hours. Inspection by optical microscopy revealed no porous features or cracks in the samples. The grains were of submillimeter size, as for typical polycrystalline samples. Several studies were also made for different annealing times. It had been demonstrated earlier that the polycrystalline nature of the samples did not influence transport measurements (*8, 14–16*). The *i*-phase structure of the samples was confirmed by powder x-ray diffraction with CuKα radiation (Fig. 1). The diffraction peaks or maxima can be completely labeled by the all-even or -odd icosahedral indices of a (six-dimensional) face-centered icosahedral crystal (*3, 4*). The high structural quality is evident from the large number of resolvable diffraction peaks (*13*). However, as noted (*9*), structural characterization is a necessary but not sufficient step for revealing intrinsic transport properties. Resistivity was measured from ~0.45 K to 290 K by means of the standard four-probe technique. Hall effect measurements were made with the six-lead method, in fields up to 4 T, at selected temperatures from 4.2 K to 290 K. Specific heat measure-

Table 1. Resistivity data on polycrystalline icosahedral-alloy samples of Al-Pd-Re annealed for ~12 hours.

Alloy composition	Annealing temperature (°C)	ρ(290 K) (μohm-cm)	ρ(4.2 K)/ρ(290 K)
$Al_{70}Pd_{20}Re_{10}$	900	~10,000	28
$Al_{70.5}Pd_{20}Re_{9.5}$	910	~11,000	12
$Al_{70.5}Pd_{19.5}Re_{10}$	900	~10,800	8.4
$Al_{70}Pd_{20.5}Re_{9.5}$	900	~8,000	4.7

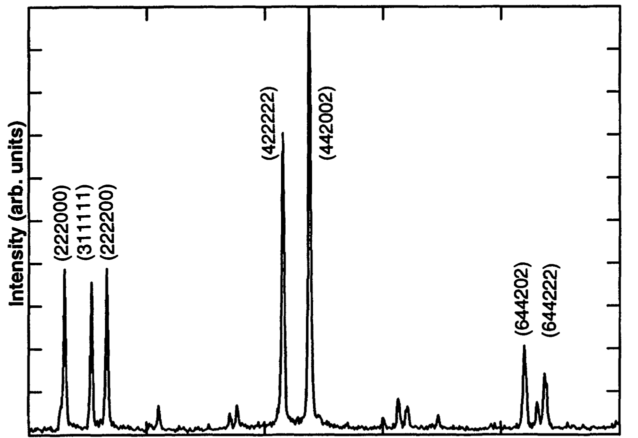

Fig. 1. CuKα powder x-ray diffraction pattern of *i*-$Al_{70}Pd_{20}Re_{10}$. Peaks are labeled according to the six-dimensional indices mentioned in the text. Due to space limitations, only intense peaks are labeled.

Department of Physics, University of Virginia, Charlottesville, VA 22901.

*To whom correspondence should be addressed.

ments were carried out on $\sim$0.2 g samples with the thermal relaxation method at temperatures from 1 K to 8 K. Experimental details, including those on high-temperature resistivity measurements up to $\sim$700°C, are to be found elsewhere (*20*).

The resistivity ratio R was found to depend on both the annealing temperature and annealing time. The largest R and ρ obtained on alloys studied are given in Table 1. Figure 2 shows $\rho(T)$ from $\sim$0.45 K to 290 K. The reproducibility of large ρ and R on different samples is high. The very rapid upturn of ρ below $\sim$10 K, resulting in $\sim$100 times increase from 290 K to 0.45 K, is reminiscent of that seen in electron insulators (*21*). To underscore this unusual behavior, a sketch of $\rho(T)$ on $Al_{65}Cu_{20}Ru_{15}$ taken from (*14*) is also shown. Clearly, the large ρ(10^5 to 10^6 μohm-cm) observed, indicates that even a very minute inclusion of a comparatively much better conductor (10 to 100 μohm-cm), less than 1% by volume, could potentially "short circuit" the intrinsic electron transport. Thus, it is not clear at this point that our results have been optimized. Further effort to purify the samples is under way. Conductivity ($\sigma = 1/\rho$) at low T (≤ 1 K) cannot be described by conduction models known for disordered metals and insulators (*10*, *21*). Rather, it appears to follow a simple power-law $\sigma \sim T^{0.5}$ on samples with $R > 10$ (Fig. 2, inset). Following the heuristic discussion on the variable-range-hopping of power law–localized electronic states $\Psi(r) \sim r^{-\alpha}$, it suggests that $\alpha \sim 0.75$, since $\sigma \sim T^{2\alpha/3}$ in the model (*9*). The measurement will be extended to the millikelvin temperature range. To learn more about the electronic structure, σ measured up to $\sim$700°C is plotted in Fig. 3. The rapid but smooth rise of σ to a nearly metallic value indicates the absence of a semiconducting gap. This feature was ascribed to the Fermi level being located near the minimum of a strong pseudogap (*9*). The strong pseudogap in ordered *i*-phases is created by the strong Fermi surface–Brillouin zone interaction (*5*, *22*) and its existence has been confirmed (*23*). In contrast, data from an Al_2Ru alloy (*24*), which is predicted to have a narrow semiconducting gap (*25*), are indeed found to be described by such a gap of $\sim$0.17 eV (Fig. 3). The two types of gaps are sketched in the inset to Fig. 3 for comparison.

Additional information on the electronic structure near the Fermi level is obtained by fitting the specific-heat data in the range $1 < T < 7$ K to the standard form $C = \gamma T + \beta T^3 + \delta T^5$ (Fig. 4). It gives $\gamma = 0.22$ mJ g^{-1} $atom^{-1}$ K^{-2} and a Debye temperature of 460 K. The γ value is much smaller than that of Al (1.35 mJ g^{-1} $atom^{-1}$ K^{-2}) but comparable to those previously reported for *i*-phases (*14*, *15*). The latter can also be said about the Hall coefficient (inset to Fig. 4), particularly in its strong T-dependence which was also interpreted by the pseudogap mechanism (*9*). The Hall coefficient is independent of the magnetic field. The effective number of hole-like carriers is estimated to be $\sim 10^{20}$ cm^{-3} at 4.2 K. Based on the electron density, the Al-Pd-Re alloys may just be semimetals. However, the data combine to suggest that these *i*-phases are quasiperiodic insulators, possibly of the Anderson type.

The present results naturally raise several questions: Why weren't the ordered *i*-phases studied previously insulators, given their comparable electron densities to the current ones? Why is a real gap not seen in ordered *i*-quasicrystals, given the prediction for its existence due to the creation of gaps around the almost isotropic Brillouin zone boundaries (*19*)? In contrast, the com-

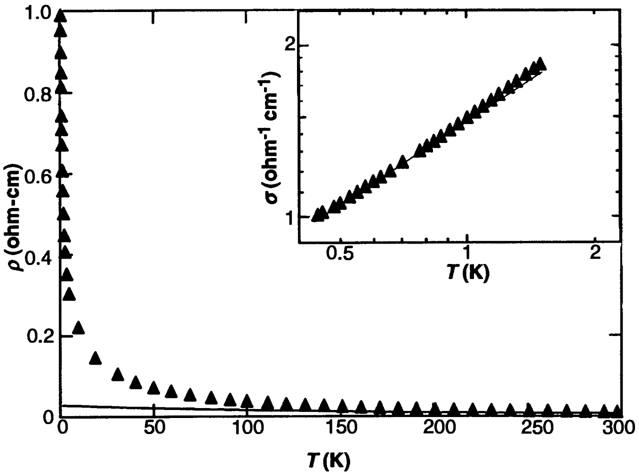

Fig. 2. Resistivity versus temperature for the *i*-$Al_{70}Pd_{20}Re_{10}$ samples that reach $\sim$1 ohm-cm at $T = 0.45$ K (▲), also shown is a sketch of $\rho(T)$ in *i*-$Al_{65}Cu_{20}Ru_{15}$ for comparison (*24*). Inset: log(σ) versus log T. The straight line illustrates the power law appearance of data at $T <$ 1 K alluded to in the text.

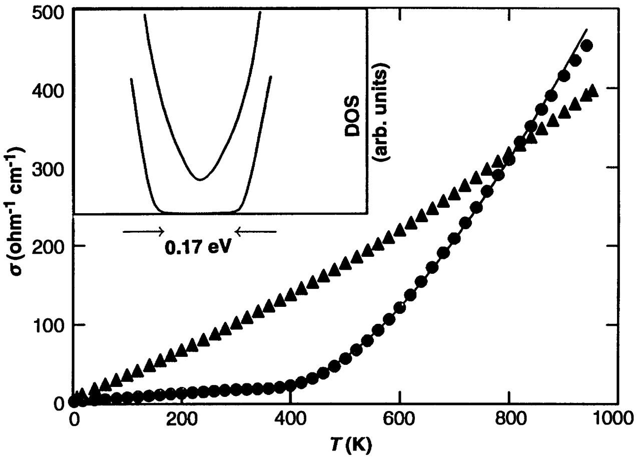

Fig. 3. Conductivity versus temperature scans of *i*-$Al_{70}Pd_{20}Re_{10}$ (▲) and Al_2Ru compound (●). The solid line drawn is a trace of the dependence $e^{-E_g/kT}$ *where* $E_g \sim 0.17$ eV is the gap (*24*). The inset illustrates the two types of gaps alluded to in the text.

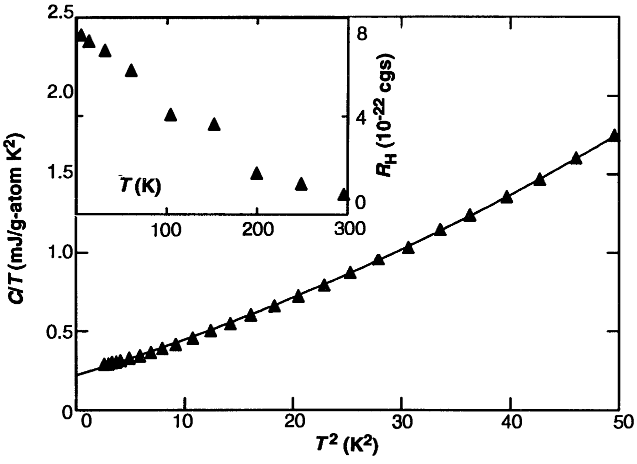

Fig. 4. Specific-heat data plotted in the form *C/T* versus T^2. The solid line is a fit to the expression $C = \gamma T + \beta T^3 + \delta T^5$ where $\gamma = 0.22$ mJ g^{-1} $atom^{-1}$ K^{-2}, $\beta = 0.020$ mJ g^{-1} atom K^{-4}, and $\delta = 2.1 \times 10^{-4}$ mJ g^{-1} $atom^{-1}$ K^{-6}. The inset shows Hall coefficient versus temperature.

pound Al_2Ru which is orthorhombic and has comparable strength of atomic potential to the *i*-phases, does have a real gap. It is mentioned above that electrons in a quasiperiodic lattice are prone to localization [also see (*26*)], and the extent of the effect depends on the form of the atomic potential in an alloy. Meanwhile, whether the absence of a real gap is also due to "quasiperiodicity" needs to be investigated. Taking a different viewpoint, an internal structural model (*27*) advocates that in the ordered *i*-phases, the icosahedral atomic blocks that are metallic, are enveloped by a layered-structure network that is insulating with an energy gap. This structural arrangement leads to a proximity tunneling type of conductivity with a finite density of states at the Fermi level. Clearly, much research is needed for understanding electron localization and band-gap formation in metallic quasicrystals as well as ordered metallic systems in general.

REFERENCES AND NOTES

1. D. Shechtman *et al., Phys. Rev. Lett.* **53**, 1951 (1984).
2. D. Levine and P. J. Steinhardt, *ibid.*, p. 2477.
3. D. P. DiVincenzo and P. J. Steinhardt, Eds., *Quasicrystals: The State of the Art, Directions in Condensed Matter Physics, vol. 11* (World Scientific, Singapore, 1991).
4. P. W. Stephens and A. I. Goldman, *Sci. Am.* **264**, 44 (April 1991); A. I. Goldman and M. Widom, *Annu. Rev. Phys. Chem.* **42**, 685 (1991). These provide tutorials on the indexing of icosahedral crystals.
5. T. Fujiwara and H. Tsunetsugu, in (*3*), p. 343.
6. H. Hiramoto and M. Kohmoto, *Int. J. Mod. Phys. B* **6**, 281 (1992).
7. L. S. Levitov, *Europhys. Lett.* **7**, 343 (1988); M. Kohmoto and H. Hiramoto, *Int. J. Mod. Phys. B*, in press. As in (*5*) the models are one- and two-dimensional. However, it was speculated that the key features noted could be extrapolated to three dimensions.
8. K. Kimura and S. Takeuchi, in (*3*), p. 313.
9. S. J. Poon, *Adv. Phys.* **41**, 303 (1992).
10. P. A. Lee and T. V. Ramakrishnan, *Rev. Mod. Phys.* **57**, 287 (1985); also articles in *Electron-Electron Interactions in Disordered Systems*, edited by A. L. Efros and M. Pollak (North-Holland, Amsterdam, 1985). It should be pointed out that there is a class of cerium and uranium metallic compounds known as Kondo insulators that exhibit semiconducting behavior, apparently ascribable to the formation of a spin gap. See for example, G. Aeppli and Z. Fisk, *Comm. Condens. Matter Phys.* **16**, 155 (1992).
11. P. A. Heiney *et al., Science* **238**, 660 (1987).
12. For a review, see A. P. Tsai *et al.*, in *Physics and Chemistry of Finite Systems: From Clusters to Crystals*, NATO ASI Series, P. Jena, S. N. Khanna, and B. K. Rao, Eds. (Kluwer, Boston, 1992), vol. I, p. 39.
13. C. Guryan *et al., Phys. Rev. Lett.* **62**, 2409 (1989); P. Bancel, *ibid.* **63**, 2741 (1989); A. R. Kortan *et al., ibid.* **64**, 200 (1990).
14. AlCuRu, ~30,000 μohm-cm, $R \sim 4$. [B. D. Biggs, S. J. Poon, N. R. Munirathnam, *ibid.* **65**, 2700 (1990).]
15. AlCuFe, ~10,000 μohm-cm, $R \sim 2.3$. [T. Klein *et al., ibid.* **66**, 2907 (1991); also T. Klein *et al., Europhys. Lett.* **13**, 129 (1990).]
16. AlPdMn, ~ 9,500 μohm-cm, $R \sim 2$. [P. Lanco *et al., Europhys. Lett.* **18**, 227 (1992).]
17. AlPdRe, ~120,000 μohm-cm, $R \sim 10$. (K. Edagawa *et al.*, unpublished results.)
18. C. C. Homes *et al., Phys. Rev. Lett.* **67**, 2694 (1991).
19. A. E. Carlsson, *Nature* **353**, 15 (1991); *Phys. Rev. B* **47**, 2515 (1993).
20. J. L. Wagner *et al., Phys. Rev. B* **38**, 7436 (1988); B. D. Biggs, thesis, University of Virginia (1992).
21. N. F. Mott, *Conduction in Non-Crystalline Materials* (Oxford Univ. Press, New York, 1987). The conduction models include those based on the variable range hopping and scaling theories.
22. A. P. Smith and N. W. Ashcroft, *Phys. Rev. Lett.* **59**, 1365 (1987); V. G. Vaks, V. V. Kamyshenko, G. D. Samolyuk, *Phys. Lett. A* **132**, 131 (1988); J. Freidel, *Helv. Phys. Acta* **61**, 538 (1988).
23. A. Sadoc *et al., J. Non-Cryst. Solids* **153 & 154**, 338 (1993); E. Belin, in (*12*), p. 829.
24. F. S. Pierce and S. J. Poon, unpublished results. In view of the fact that the states near the Fermi level are localized, the rapid rise in conductivity above ~400 K is determined by the activation of these states into the conduction band. Since the Fermi level is located near the top of the valence band, the use of $\rho \propto e^{E_g/k_BT}$ is appropriate.
25. D. N. Manh *et al., Solid State Commun.* **82**, 329 (1992).
26. A. Yu. Kitaev, *Sov. Phys.–JETP Lett.* **48**, 298 (1990).
27. J. C. Phillips and K. M. Rabe, *Phys. Rev. Lett.* **66**, 923 (1991).
28. This work was supported by National Science Foundation contract DMR90-15538.

9 April 1993; accepted 11 June 1993

Thorium-Uranium Fractionation by Garnet: Evidence for a Deep Source and Rapid Rise of Oceanic Basalts

T. Z. LaTourrette,* A. K. Kennedy,† G. J. Wasserburg

Mid-ocean ridge basalts (MORBs) and ocean island basalts (OIBs) are derived by partial melting of the upper mantle and are marked by systematic excesses of thorium-230 activity relative to the activity of its parent, uranium-238. Experimental measurements of the distribution of thorium and uranium between the melt and solid residue show that, of the major phases in the upper mantle, only garnet will retain uranium over thorium. This sense of fractionation, which is opposite to that caused by clinopyroxene-melt partitioning, is consistent with the thorium-230 excesses observed in young oceanic basalts. Thus, both MORBs and OIBs must begin partial melting in the garnet stability field or below about 70 kilometers. A calculation shows that the thorium-230–uranium-238 disequilibrium in MORBs can be attributed to dynamic partial melting beginning at 80 kilometers with a melt porosity of 0.2 percent or more. This result requires that melting beneath ridges occurs in a wide region and that the magma rises to the surface at a velocity of at least 0.9 meter per year.

Information about the rate at which a source region melts and the magma is transported to the surface of the Earth can provide key constraints on magmatic plumbing systems in the mantle and crust. One important source of this information is isotopic disequilibrium among the members of the uranium-series decay chain in young oceanic basalts. Most young MORBs and OIBs display secular disequilibrium between ^{230}Th and ^{238}U, with the activity of ^{230}Th enriched relative to that of ^{238}U (*1*). This disequilibrium implies that the basalts have a higher Th/U ratio than the mantle from which they were derived. Such a Th-U fractionation generates a transient excess of ^{230}Th relative to its parent, ^{238}U, in the basalt. Because a system will return to secular equilibrium (where the ^{230}Th and ^{238}U activities are equal) within about five half-lives of ^{230}Th (or 377,000 years), ^{230}Th-^{238}U disequilibrium reflects recent chemical fractionation of Th from U and can be used to constrain the timing of magma generation and transport. In order to interpret this disequilibrium, however, the origin of the Th-U fractionation, that is, the location and the time in the erupted lava's history when the fractionation occurred, must be determined.

Many workers have attributed the Th-U fractionation to differences in crystal-melt partitioning between Th and U during partial melting (*1–3*). Recent experimental trace-element partitioning studies have shown that partial melting of spinel lherzolite is not a possible explanation of ^{230}Th-^{238}U disequilibrium in young oceanic basalts, as a partial melt from such a source will be enriched in U relative to Th, which is opposite to what is found (*4, 5*). This conflict could be resolved if partial melting occurred at higher pressures where other phases controlled the Th and U partitioning. We thus conducted partitioning experiments between garnet and melt to evaluate the possibility that ^{230}Th-^{238}U disequilibri-

Division of Geological and Planetary Sciences, California Institute of Technology, Pasadena, CA 91125.

*To whom correspondence should be addressed at Department of Geology, Box 1404, Arizona State University, Tempe, AZ 85287.

†Present address: Department of Applied Physics, Curtin University of Technology, Perth, 6001, Australia.